Laser Propagation in an Underwater Environment

Charles Stabler, MIDN USN
United States Naval Academy Weapons and Systems Engineering Department
m176150@usna.edu

Gabe Collins, MIDN USN
United States Naval Academy Weapons and Systems Engineering Department
m171170@usna.edu

Abstract: From a naval warfare perspective, lasers have useful applications such as the LaWS on the USS Ponce or wireless communication between a submarine and an ROV. Beam propagation in a maritime environment presents hindrances to the beam's integrity. Experimentation was performed with four different beam types from a 2 mW HeNe laser into a water tank filled with non-potable water in both calm and turbulent scenarios. The beam types are unexpanded, expanded, and two spatial light modulated beams that differ in coherence. Both the scattering and propagation views are observed, and the relative intensity and scintillation index are measured of all four beams from both views. The relative intensity and scintillation index are determined to evaluate which measure allows for the best detection of each type of beam. What follows are initial results.

From the scattering perspective, the more coherent beam maintains a higher relative intensity and less scintillation than the less coherent beam in both calm and turbulent scenarios; and the expanded beam has less change in both relative intensity and scintillation index for each scenario. From a propagation perspective, the more coherent beam scintillates less than the less coherent beam while the unexpanded and expanded beams have no measurable difference in scintillation index for each scenario. Due to the differences in intensities between the Gaussian and spatially modulated beams, drawing conclusions to detection based on relative intensities would require further experimentation.

1. Introduction

This experiment sought to explore how to best detect different types of red wavelength laser beams in an underwater environment, and how spatial light modulated beams penetrate an underwater medium compared to unexpanded and expanded beams. Two different coherent values of spatial light modulated beams were tested against the two traditional beams. In the experiment, two water turbidity scenarios are used to provide different levels of impedance to the beams' propagation. To analyze the best options for detecting a beam underwater, two different views of the beams tell different stories.

2. Motivation

With directed energy applications becoming less of a rarity in Naval Applications as they have been, it is now more important than ever to be able to detect a beam as it propagates through a medium. Wireless optical communication underwater enables much higher data transmission rates than wireless acoustic communication, making underwater optics research valuable to the military, scientific, and commercial communities [1,2]. Countries such as the United States, China, and Germany have participated in research in the field of laser communications, examples of which are shown in Figures 1 and 2 [3,4]. In order to intercept laser communications, an adversary would first have to locate the path of propagation in order to intercept the information traveling via the laser beam. Blocking the beam from propagating is another option to interrupt communications or serve as a defensive measure to a weaponized beam. Observing the scattering of such a beam may be an effective tool in order to accomplish the task of beam location. If targeted by a weaponized laser beam, a more appropriate form of detection of that attack may be observing the propagation directly. By propagating a beam underwater, observations can be made concerning the potential effectiveness of laser communications or weaponized lasers.

Fig. 1 Applications of lasers in a maritime environment. The left picture shows a German experiment in underwater laser communication; the right shows the LaWS on the USS Ponce [3].

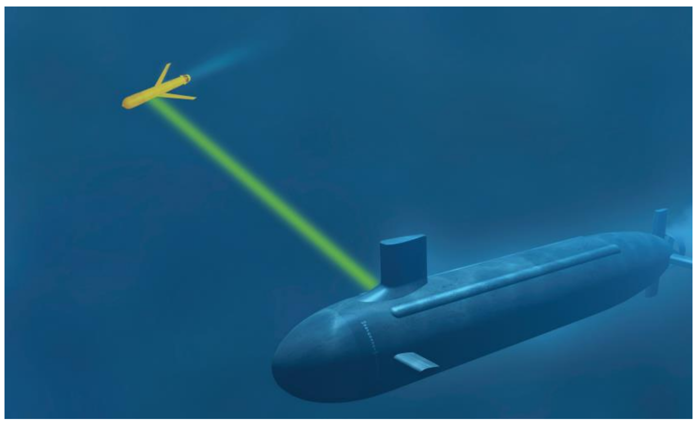

Fig. 2 Visualization of underwater wireless communications using optics between an AUV and a submarine. Image from SA Photonics

3. Procedure and Setup

For this series of experiments, a large tank was used as the testing environment of propagation of four different types of beams. The beam source used was a 2 mW red laser with a wavelength of 632.8 nm and a diameter of 0.63 mm at the source. This source was not chosen to most easily pass through water with the least amount of scattering, but it was an effective tool to observe scattering [5]. Upon leaving the source, the beam was directed using a series of mirrors in order to orient the beam in such a way that it would enter the water tank perpendicular to the tank's vertical surface. For the expanded scenario, a 10x expander was used. For the modulated beam types, the beam first hit a Spatial Light Modulator (SLM) before being directed by a series and mirrors, and an iris was used to isolate one specific beamlet in order to stop the others from interfering with results.

The function of spatial light modulator in this experiment, simply, is to create a "flat-top" beam; meaning that the beam profile is more rectangular than the normal Gaussian profile. A spatial light modulator performs phase or amplitude modulation of a laser beam using an array of liquid crystals that are electronically controlled by applying voltages across the array. "Screens" are created (in this case, using Matlab) and applied to the array of liquid crystals that the spatial light modulator uses to shape the beam. In the experiment, the beam was directed at the spatial light modulator, which reflected multiple Gaussian beamlets to recreate the single desired "flat-top" beam. The original beam, in addition to being spatially modulated, was temporally modulated by rapidly changing the screens.

Ultimately, the spatial light modulator (SLM) creates a spatially, partially coherent, multi-gaussian shell beam. The experiment focused on the multi-gaussian and shell portion of the beam. The “less coherent” beam consists of 30 beamlets, and the “more coherent” beam consists of 60 beamlets. With a higher number of beamlets, the edges of the beam are more defined. The shells are how temporal modulation is achieved: by changing the screens rapidly, “shells” of the multi-gaussian beamlets are created.

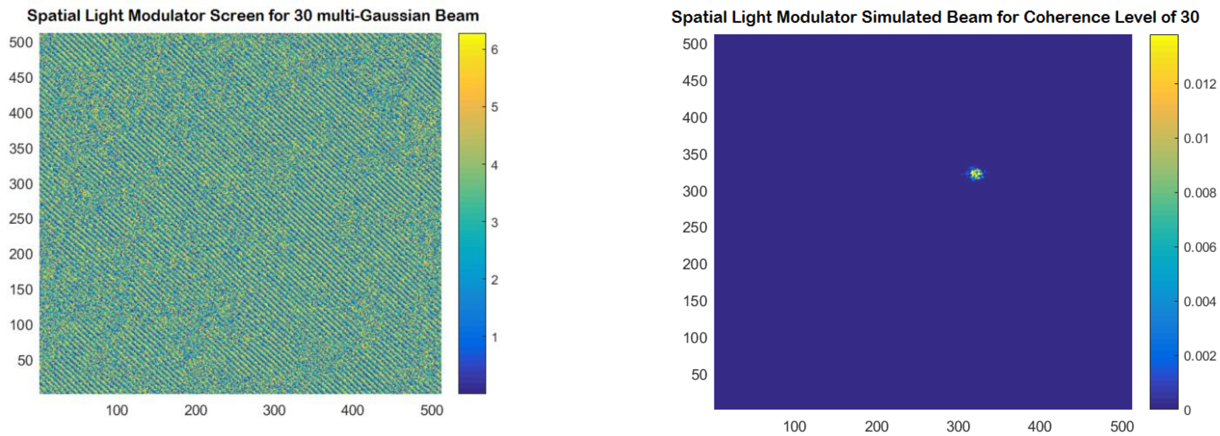

Fig. 3 Example of screen that the spatial light modulator creates on the liquid-crystal array and how the resultant beam appears.

Each scenario was documented using both a side view camera to capture scattering and a direct view camera to capture propagation. The side, or scattering, view camera was located 65 cm away from the beam, used a 75 mm lens, and had a 14.4 cm field of view of the beams. The direct, or propagation, view camera was located directly at the end of the tank to capture the beam as it exited the tank. The unexpanded and expanded beams propagated 4.3 m before entering the tank, and the SLM beams propagated 5.4 m before entering the tank. The water tank was 2.5 m long; for a total propagation distance of 6.8 m and 7.9 m, respectively. A neutral density filter with a power of 1.6 and a red light filter were used on the direct view camera. The direct view camera took pictures at a rate of one picture per 30 ms. Observations of the beam from the direct view occurred at half the rate that the SLM changed screens to restructure the beam in order to minimize scintillation due to the changing screens. The side view camera took pictures at a rate of one picture per 500 ms. A difference between the image capture rate is owed to the long exposure necessary for the scattering view camera to observe the beams. Each scenario was captured over a 500 frame period, for a total capture time of 15 seconds from the propagation view and 250 seconds from the scattering view. A water pump was used in order to create our turbulent environment, with non-potable fresh water used in the tank; and 30 minutes was allowed to establish a stable environment when switching between the turbulent and calm scenarios.

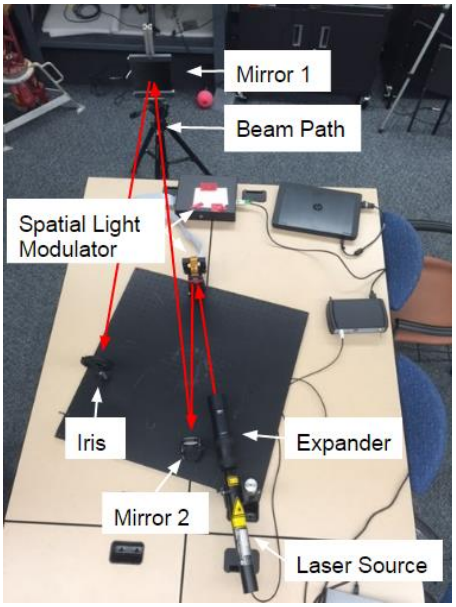

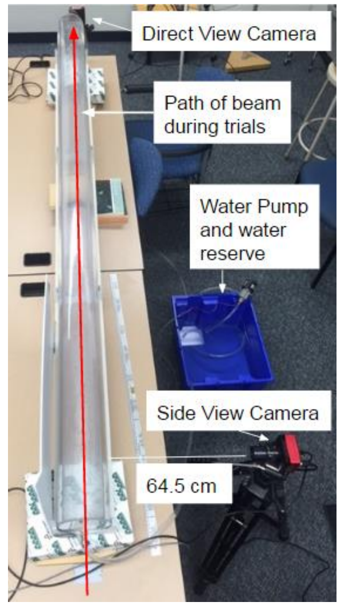

Fig. 4 Lab setup of laser propagation path before entering the tank, and the propagation into the tank.

4. Results and Analysis

With the setup of the experiment, the relative intensity of the different beams could be measured, and from that, the scintillation index and beam size from a scattering perspective could be calculated. Values for "relative intensity" are simply unitless pixel values that the camera measures, and the cameras have the ability to measure 2^{14} distinct values per pixel. Comparisons of each scenario were analyzed to determine effective ways for detecting each type of beam for the scenarios.

Table 1 Numbering the beam types and different scenarios for reference throughout the paper

Beam Type	Beam Number
Unexpanded	1
Expanded	2
SLM less	3
SLM more	4

Scenario	Scenario Number
Calm	1
Turbulent	2

Image processing and calculation of mean, variation, and scintillation was accomplished with Matlab. For a series of images of one beam type during a scenario, the mean relative intensity and variance of each pixel was calculated. Scintillation of a pixel is calculated using the following equation, where σ^2 is variance and μ is mean:

$$S = \frac{\sigma^2}{\mu^2} \ . \qquad (1)$$

```
%% Finding mean, variance, and scinitillation index of each pixel

FIexp = double(FIexp); % change data type of image matrices
mmatexp = zeros(nImage,mImage); % create empty matrix for mean relative intensity
vmatexp = zeros(nImage,mImage); % create empty matrix for variance
simatexp = zeros(nImage,mImage); % create empty matrix for scintillation

% sort through all image matrices; calculate mean, variance, and
% scintillation for each pixel and recreate into matrix.
for ii=1:nImage
    for jj=1:mImage
        mmatexp(ii,jj) = mean(FIexp(ii,jj,:));
        vmatexp(ii,jj) = var(FIexp(ii,jj,:));
        simatexp(ii,jj) = vmatexp(ii,jj)/mmatexp(ii,jj)^2;
    end
end

```

Fig. 5 Example code for calculating mean, variance, and scintillation for the images in Matlab.

For more clarification on the effect that the different scenarios have on the beams, the intensities of Beams 1 and 2 are compared for both scenarios in Figure 6, and the same for Beams 3 and 4 in Figure 7. These images were taken from the scattering perspective. The images show that in Scenario 2, more light reaches the camera sensor due to greater scattering; with the exception of Beam 2. Also, for Beams 3 and 4, the difference between beam structure appears. Beam 4 appears wider due to the greater number of Gaussian shells than Beam 3.

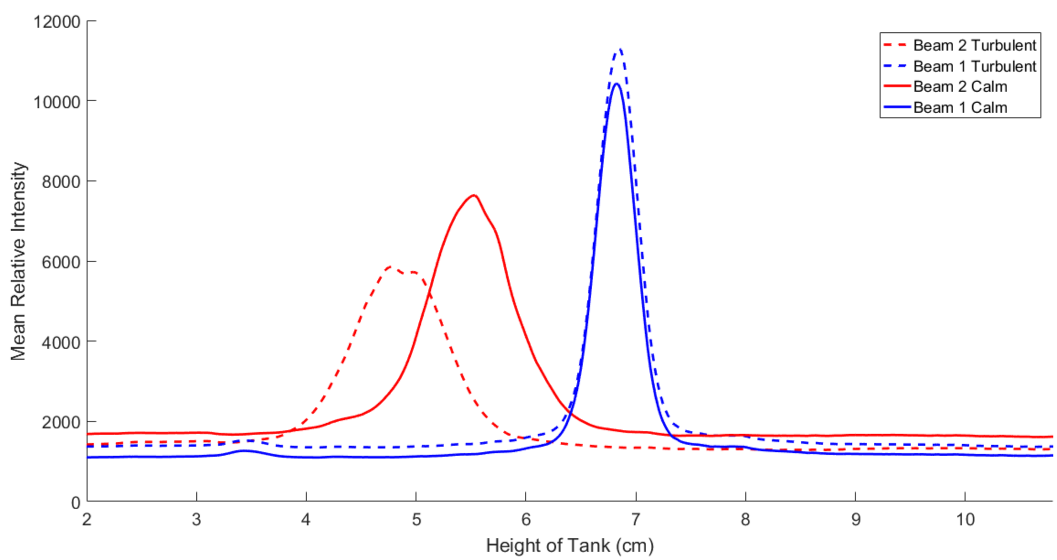

Fig. 6 Scattering perspective, mean relative intensity across the field of view for Beams 1 and 2. Notice for Beam 2 that the intensity for the calm scenario is higher than that of turbulent scenario; an unexpected result.

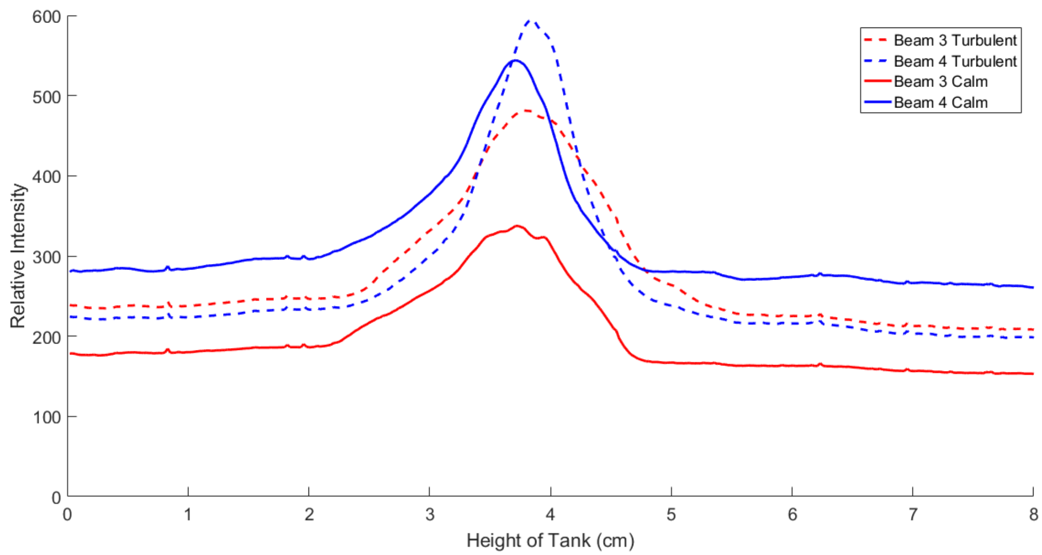

Fig. 7 Scattering perspective, mean relative intensity across the field of view for Beams 3 and 4. This is also a good visualization of the difference in beam structure between the more coherent and less coherent beam.

5. Scenario 1

This scenario was used as a baseline to obtain expected results for Scenario 2, as the latter is a more realistic environment for applications. From the scattering perspective, the average relative intensity value for each pixel was used to create one frame for observation and analysis.

Table 2 Results of Scenario 1 comparing relative intensity at the entrance and exit of field of view to each other and to the background intensity.

Scenario 1 Results			
Beam Number	Relative Intensity Retained (%)	Entrance Intensity Compared to Background Intensity	Exit Intensity compared to Background Intensity
1	51	12.2	6.2
2	57	6.1	3.5
3	70	3.2	2.2
4	63	3.2	2

Overall trends of the results presented in Table 2 are that the unexpanded and expanded beams have a much higher relative intensity than the SLM beams (Beams 3 and 4), though the SLM beams retained a larger percentage of their intensity after propagation over the field of view. The percentages are simply a comparison of the unitless pixel values that the camera measures at the entrance and exit of the field of view. For Beams 3 and 4, the difference between the relative intensities of the beam and the medium was that at the entrance of the field of view, the beams were approximately 3 times the intensity of the medium (or background) and 2 times at the exit. The Beam 2 was 12 times the intensity of the background at the entrance and 6 times at the exit; while Beam 1 was 6 times the background intensity at the entrance and 3.5 times at the exit. These results suggest that a sensor that has the ability to measure light intensity and discriminate differences in intensity would be effective in observing all four types of beams, though this sensor would be most effective in detecting unexpanded and expanded beam types.

From the series of frames captured, the scintillation index for each pixel was calculated and presented as one frame. Overall trends were that Beams 3 and 4 had higher scintillation values and greater change in scintillation than Beams 1 and 2 as shown in Figure 9. However, the scintillation values for all four beam types are below 0.15, with the values of the scintillation of the beams being 0.02 and within a range of ± 0.01. In calm water, it follows that the scintillation would not be the most effective way of detecting beams.

The propagation perspective portrayed a similar story as the scattering perspective. For Beams 1 and 2, the relative intensity was higher and the scintillation was lower than Beams 3 and 4, shown in Figure 10. For the scintillation, the expanded and unexpanded beams averaged about 0.25 while Beams 3 and 4 averaged about 0.30 in Figure 11. The greater scintillation values and differences in scintillation make this a better method for detecting beams directed at the sensor.

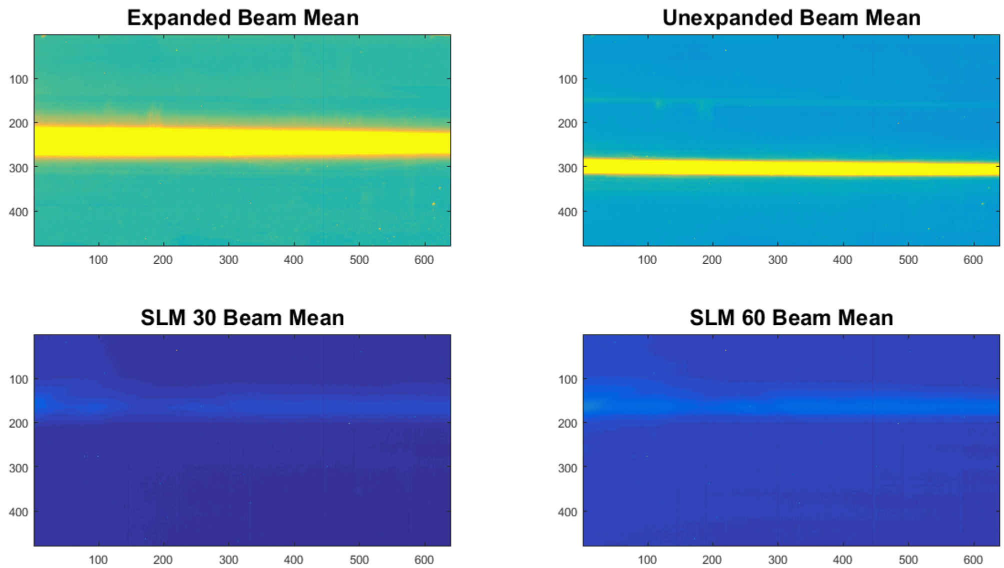

Fig. 8 Calm scenario scattering view relative intensities

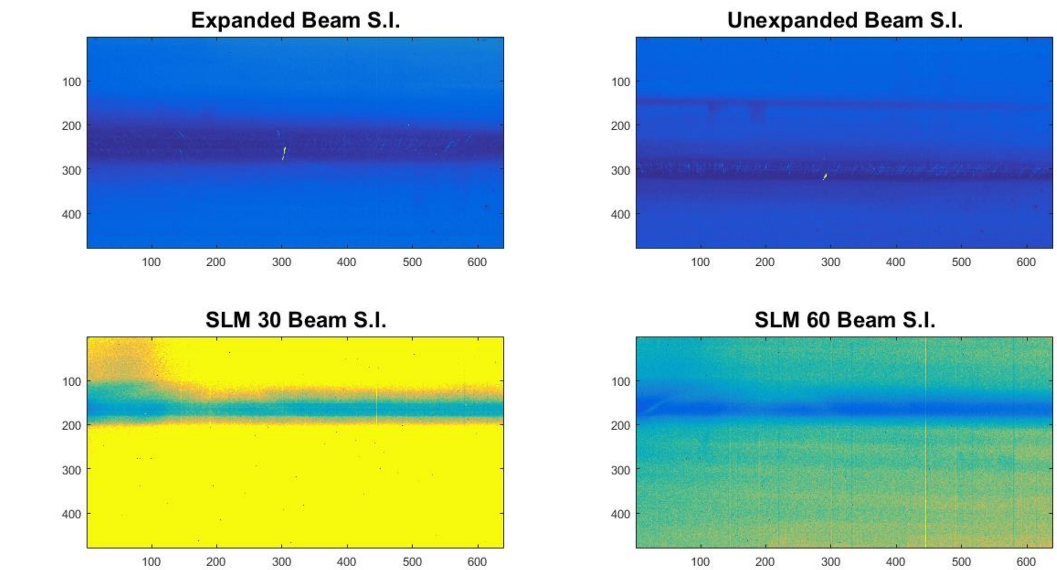

Fig. 9 Calm scenario scattering view scintillation indices

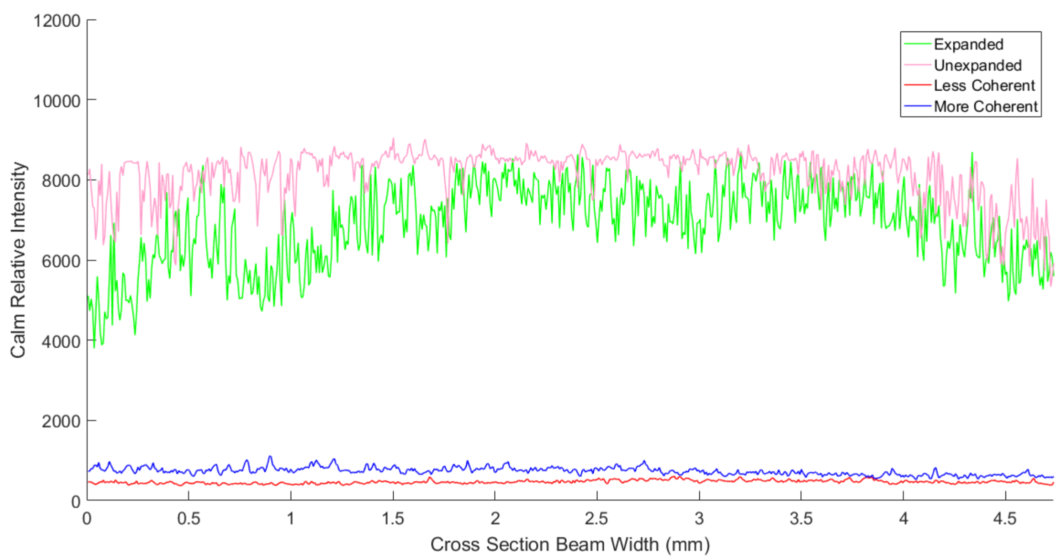

Fig. 10 Calm scenario propagation view relative intensities

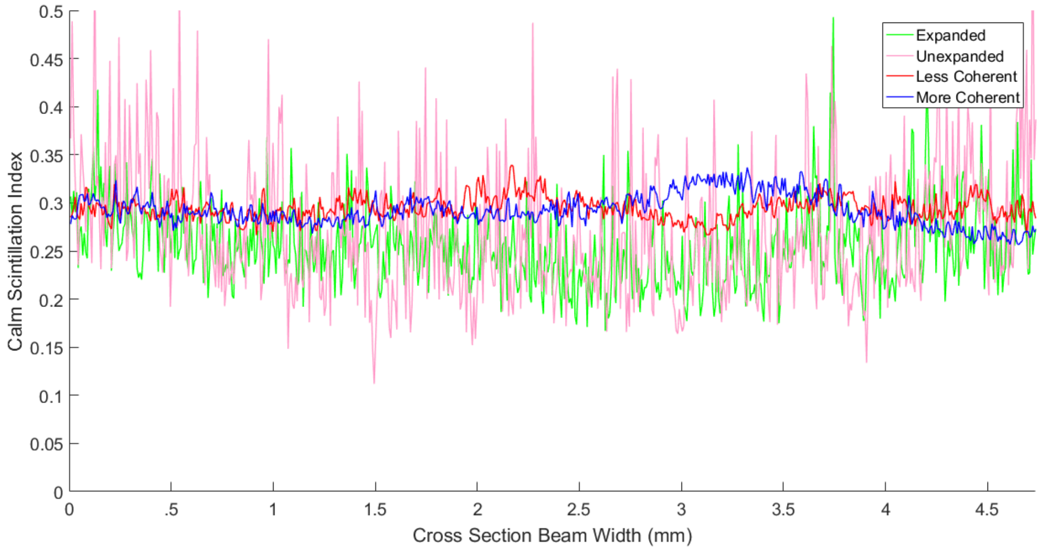

Figure 11 Calm propagation view scintillation indices

6. Scenario 2

This scenario created an environment that was closer to what a laser would actually encounter in the real world, with the churning water simulating waves and currents. In the experiment, a small 12 volt pump was used to maintain a flow into the end of the tank away from the beam entrance to the tank. To achieve similar turbidity among experiments, calm measurements (Scenario 1) were taken first, then the pump was turned on and left running for 30 minutes before the Scenario 2 measurements were taken. This time period allowed water turbidity throughout the length of the tank. The same methods as used in Scenario 1 were used to analyze this scenario.

Table 3 Results for Scenario 2 comparing relative intensity at the entrance and exit of field of view to each other and to the background intensity.

Scenario 2 Results			
Beam Number	Relative Intensity Retained (%)	Entrance Intensity Compared to Background Intensity	Exit Intensity Compared to Background Intensity
1	57	10.8	6.2
2	57	6	3.5
3	67	2.9	2
4	62	4.1	2.5

In terms of relative intensity, Beams 1 and 2 again have a higher overall intensity, but beam behavior in the medium continued to allow determination of detection methods. The relative intensity of Beam 1 was 11 times the medium's intensity at the exit and 6 times at the exit; Beam 2 measured 6 times at the entrance and 3 times at the exit; and Beams 3 and 4 measured about 4 times the background intensity at the entrance and 2 times at the exit. These results are very similar to the results of the calm scenario in that a light sensor that discriminates light intensities of the field of view would be effective for all four types of beams, with Beams 3 and 4 being less obvious to the sensor. Figure 12 shows the scattering view of the beams in terms of relative intensity.

The scintillation index of the beams in Scenario 2 follows a different trend than that of Scenario 1. Scintillation values of Beams 1, 3 and 4 were between 0.02 and 0.04 from field of view entrance to exit. The Beam 4 had scintillation values between 0.02 and 0.03. The greatest change between background scintillation and beam path scintillation occurred with Beam 2 and the least change occurred with Beam 4. To detect beams based upon scintillation values, a detection system would look for areas of low scintillation in areas of relatively higher scintillation.

From the propagation perspective in the turbulent scenario, Beams 3 and 4 have higher scintillation value of approximately 0.25 compared to Beams 1 and 2 at 0.13, shown in Figure 14. This could be due to the temporal modulation of the SLM beams against the camera's exposure time. Again, as in Scenario 1, the scintillation index values would be useful to detect beams aimed directly at the sensor.

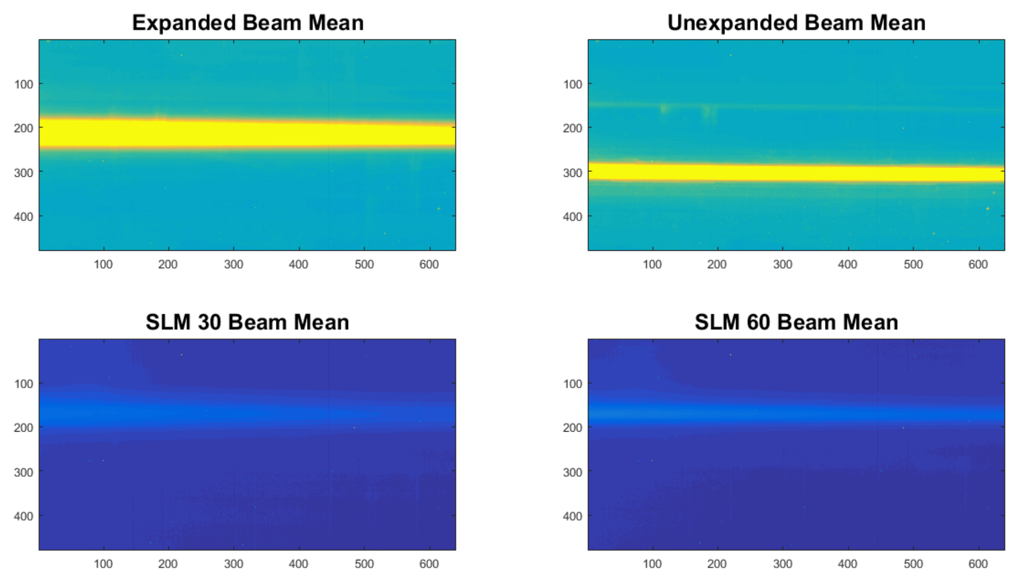

Fig. 12 Turbulent scenario scattering view relative intensities

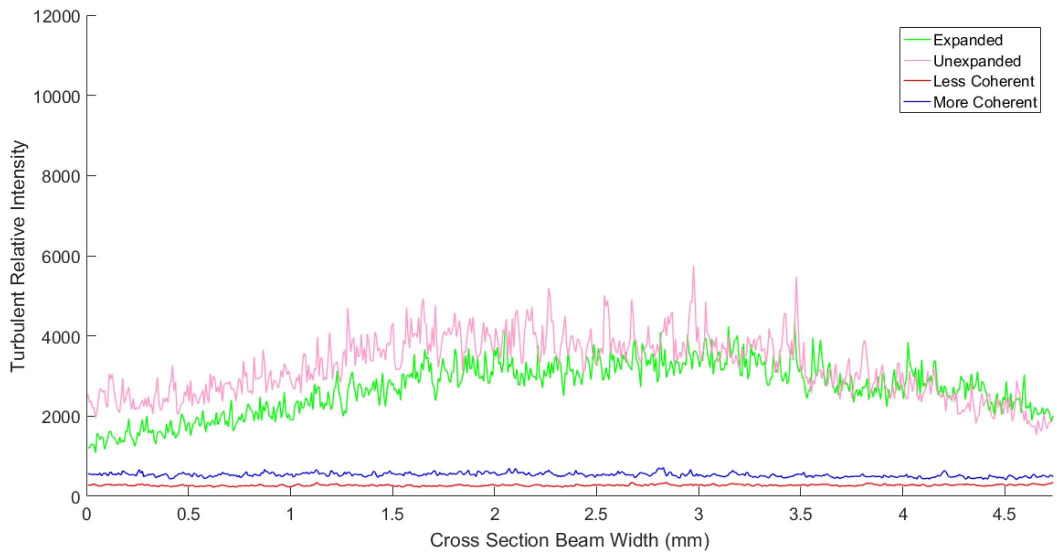

Fig. 13 Turbulent scenario propagation view means

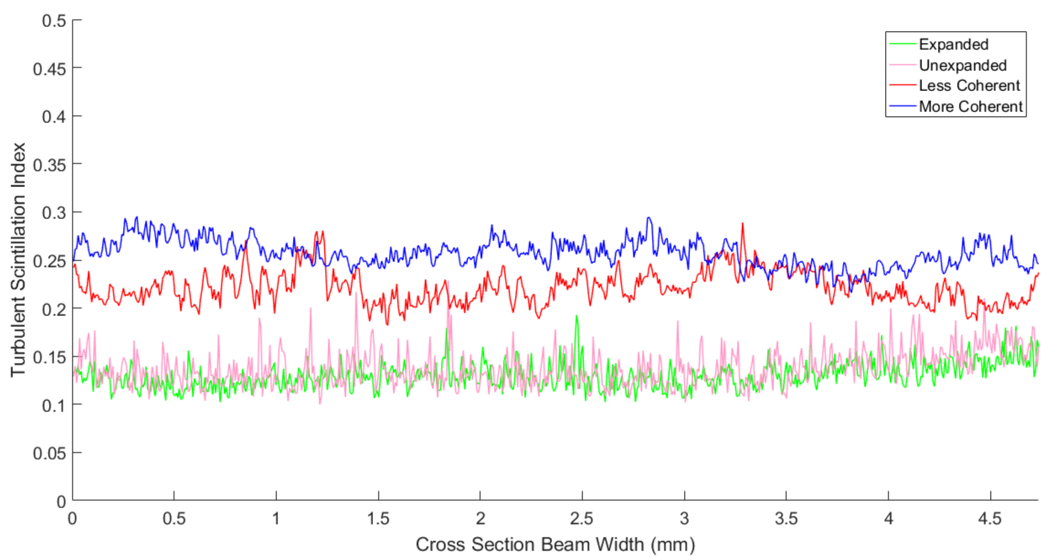

Fig. 14 Turbulent scenario propagation view scintillation indices

From the scattering perspective, the scintillation indices were measured at four points along the field of view to examine path difference. In Figures 15 through 17, Beams 2, 3, and 4 are examined. Beams 3 and 4 have a higher average values along the beam path, though Beam 2 has a wider path. In examining scintillation as a form of detection, Beam 2 would present the easier beam to observe because of the large abnormality that it presents compared to the medium. Although Beams 3 and 4 have greater difference in value, their propagation path is smaller than Beam 2. Beam 4 has the smallest path size, though the greatest difference between background and path scintillation values.

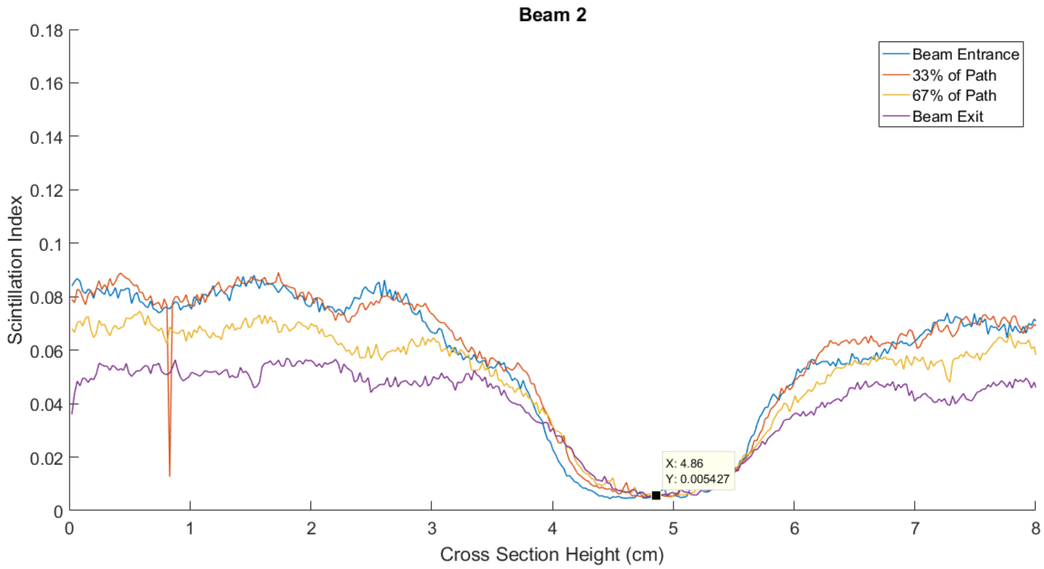

Fig. 15 Scenario 2 scattering view scintillation indices of Beam 2

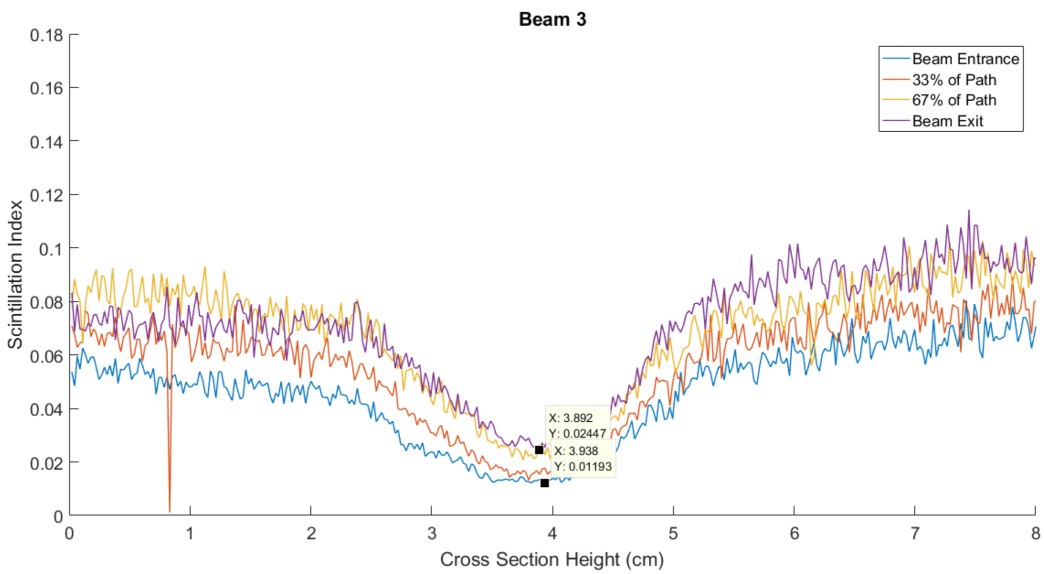

Fig. 16 Scenario 2 scattering view scintillation indices of Beam 3

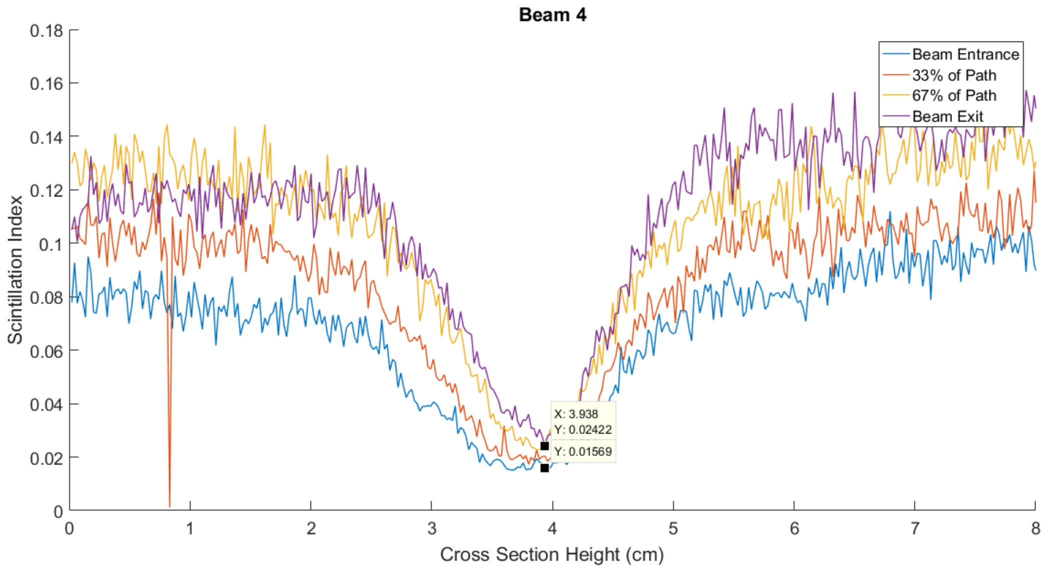

Fig. 17 Scenario 2 scattering view scintillation indices of Beam 4

7. Conclusion

The results of the experiment are a mix of expected and unexpected. In Scenario 1, Beams 3 and 4 had a higher scintillation values than Beams 1 and 2. In Scenario 2, Beam 4 scintillated the least of the SLM beams, as expected. In terms of detection, this experiment reviewed if detecting beams by measuring relative light intensity or scintillation index values from a scattering view, as in observing communications, or a propagation view, as in defensive measure against a weaponized beam, would be most effective for accurate detection. Overall, the expanded and unexpanded beams would be effectively detected by measuring relative light intensity in a camera's field of view, and less so with the SLM beams at the current reflection percentage of the modulator. The scintillation index values could potentially work as a detection method for all beam types if comparing a potential beam to the background scintillation. A follow on for this experiment could involve propagating beams underwater on a sunny day, when the waves bend light through the water, and how those might affect beam detection.

8. References

[1] Y.-C. Chi, T.-C. Wu and C.-Y. Lin, "Underwater 6.4-m optical wireless communication with 8.8-Gbps encoded 450-nm GaN laser diode," in *Internation Semiconductor Laser Conference*, Kobe, 2016.

[2] B. Cochenour, L. Mullen and A. Laux, "Characterization of the Beam Spread Function for Underwater Wireless Optical Communcation Links," *IEEE Journal of Oceanic Engineering,* vol. 33, no. 4, pp. 513-521, 2008.

[3] T. Scholz, "Using Laser Communication Above Water and Underwater," May 2011. [Online]. Available: https://www.sea-technology.com/features/2011/0511/laser_communication.php#top. [Accessed December 2016].

[4] X. Yi, Z. Li and Z. Liu, "Underwater optical communication performance for laser beam propagation through weak oceanic turbulence," *Applied Optics,* vol. 54, no. 6, pp. 1273-1278, 2015.

[5] P. Swathi and S. Prince, "Designing issues in design of underwater wireless optical communication system," in *International Conference on Communications and Signal Processing*, Melmaruvathur, 2014.